Poly(lactic acid)-starch/Expandable Graphite (PLA-starch/EG) Flame Retardant Composites

Mfiso Emmanuel Mngomezulu[1], Adriaan Stephanus Luyt[2], Steve Anthony Chapple[3] and Maya Jacob John[3,4]*

[1]*Department of Chemistry, University of the Free State (Qwaqwa Campus), Private Bag X13, Phuthaditjhaba 9866, South Africa*
[2]*Center for Advanced Materials, Qatar University, PO Box 2713, Doha, Qatar*
[3]*CSIR Materials Science and Manufacturing, Polymers and Composites Competence Area, PO Box 1124, Port Elizabeth 6000, South Africa*
[4]*Department of Chemistry, Faculty of Science, Nelson Mandela Metropolitan University, PO Box 1600, Port Elizabeth 6000, South Africa*

Received November 01, 2016; Accepted March 11, 2017

ABSTRACT: This work reports on the effect of commercial expandable graphite (EG) on the flammability and thermal decomposition properties of PLA-starch blend. The PLA-starch/EG composites were prepared by melt-mixing and their thermal stability, volatile pyrolysis products and flammability characteristics were investigated. The char residues of the composites, after combustion in a cone calorimeter, were analyzed with environmental scanning electron microscopy (ESEM). The thermal decomposition stability of the composites improved in the presence of EG. However, the char content was less than expected as per the combination of the wt% EG added into PLA-starch and the % residue of PLA-starch. The flammability performance of the PLA-starch/EG composites improved, especially at 15 wt% EG content, due to a thick and strong worm-like char structure. The peak heat release rate (PHRR) improved by 74%, the total smoke production (TSP) by 40% and the specific extinction area (SEA) by 55%. The improvements are attributed to the ability of EG to exfoliate at increased temperatures during which time three effects occurred: i) cooling due to an endothermic exfoliation process, ii) dilution due to release of H_2O, SO_2 and CO_2 gases, and iii) formation of a protective intumescent char layer. However, the CO and CO_2 yields were found to be unfavorably high due to the presence of EG.

KEYWORDS: Poly(lactic acid)-starch composites, expandable graphite, thermal stability, flammability properties

1 INTRODUCTION

The development of biodegradable polymer composite materials with fire resistance ability and thermal stability can create new uses and extend their industrial applications. Biodegradable polymers in general and poly(lactic acid) (PLA) in particular, have recently gained considerable research interest due to environmental concerns, as well as the shortage and high cost of fossil fuel. The PLA-based composite materials possess improved chemical and physical properties when appropriate micro- and/or nanofillers, such as graphite and expandable graphite (EG) in particular, are used [1–11].

Poly(lactic acid) (PLA) is an aliphatic polyester, generally made from α-hydroxy acid. It is produced by classical synthesis using a biobased 2-hydroxy propionic acid (i.e., lactic acid) monomer. The latter can be derived from corn or potato starch, cane or beet sugar and cheese whey. PLA is applied in various fields such as medical and pharmaceuticals, textiles, packaging and composites. It is the most highly produced degradable aliphatic polyester with relatively modest cost. It has advantages that include eco-friendliness, biocompatibility, compostability, processability and energy efficiency during production. It is marred by inherent limitations, including poor thermal stability and flammability performance. Consequently, there is a need to pursue its modification through additives, such as expandable graphite, in order to achieve properties equivalent and/or superior to the conventional petroleum-based polymers [3–11].

Expandable graphite (EG) is an intercalated compound produced by the chemical or electrochemical intercalation of molecular or atom guests between the layers of graphite. Its structure consists of graphene sheets/layers within which chemical compounds (i.e., oxidants such as H_2SO_4 or HNO_3, and $KMnO_4$) are intercalated [6, 12–15]. When exposed to high

*Corresponding author: MJohn@csir.co.za

DOI: 10.7569/JRM.2017.634140

temperatures (i.e., > 190 °C), EG layers are able to exfoliate and expand rapidly in an accordion-like pattern. This is due to the decomposition of the intercalation compounds (e.g., H_2SO_4) into water and sulphur dioxide gas. EG further undergoes oxidation by H_2SO_4 with the production of carbon dioxide and sulphur dioxide gases. This exfoliation process is said to be endothermic. Thus, when used as a flame retardant in a polymer matrix, it triggers temperature decreases in the system to below the polymer combustion temperature. Since the decomposition of an acid and the redox reaction between an acid and graphite result in the production of inert gases (i.e., H_2O, CO_2 and SO_2), it leads to dilution of a mixture of combustible gases. Finally, the resultant carbonaceous intumescent char will form a protective layer between the gaseous and the solid combustible phases [16, 17]. Since EG begins to exfoliate at temperatures below the onset of thermal decomposition of PLA at ~ 280 °C, EG will act before the thermal decomposition of the biopolymer. It will therefore modify the thermal decomposition pathway of PLA to yield some char and lower the evolution of flammable pyrolysis products [6, 13, 14, 18].

A number of studies were conducted where expandable graphite was used as a flame retardant in various polymer matrices. EG was either used alone or with other additives in polymers such as polyolefins, polystyrene, epoxy, polyurethanes, polyamide and PLA [5, 12, 16, 17, 19–31]. The polymer/EG composites were generally prepared either by solution mixing, melt extrusion/blending, milling or injection molding. For instance, Xie and Qu [19, 20] investigated the synergistic effect and the thermo-oxidative degradation behavior of expandable graphite with halogen-free flame retardant additives (i.e., ammonium polyphosphate, zinc borate, phosphorus-nitrogen compounds and microencapsulated red phosphorus) in LLDPE- and EVA-based systems. It was found that the combination of EG with other flame retardant additives increased the LOI values, improved flammability performance and increased the thermo-oxidative degradation temperature while reducing the oxidation heat [19]. It was concluded that the phosphorus-nitrogen compound was an efficient synergist, whereas zinc borate acted as a smoke suppressant in the polyolefin/EG flame resistant system. The presence of EG in LLDPE [20] improved the thermo-oxidative degradation by lowering the decomposition rates. In another study by Wang *et al*. [17], the fire and water resistance of coatings, based on expandable graphite and an intumescent flame retardant additive composed of ammonium polyphosphate, pentaerythritol and melamine, were compared. It was reported that EG (with 74 μm particle size) showed better antioxidation and fire resistance properties and that EG coating (at 8.5%) retained the material's fire resistance ability, even after 500 hours of water immersion.

Focke and coworkers reported on the characterization [16] and use of expandable graphite in thermally conductive phase-change materials [21] and in fire retardant LDPE [22] and poly(vinyl chloride) (PVC) [23] systems, prepared by extrusion and high shear mixing and followed by curing at elevated temperatures. They reported that although EG more effectively lowered the smoke emission and peak heat release rate (PHRR) than the novel intumescent additive (i.e., phosphate salt of 3,5-diaminobenzoic acid) synthesized in LDPE, the combination of these two led to a further reduction in PHRR. This was attributed to the formation of a heat insulating protective barrier at the solid surface, thus limiting the heat transfer to the substrate and slowing down the material's rate of thermal degradation [22]. In the case of a PVC/EG system (where PVC was plasticized with 60 phr phosphorus ester) they found that the PHRR and total heat release (THR) were reduced with only 5 wt% EG inclusion, and they attributed it to an excellent match between the exfoliation onset temperature of EG and the onset of decomposition of the PVC [23].

Only a few studies reported on the use of expandable graphite as a flame retardant in a PLA matrix [5, 32, 33]. Wei *et al*. [5] investigated the thermal stability and combustion behavior of extruded PLA/expandable graphite composites. They reported that the PLA/EG composites showed the highest V-0 ranking (UL-94 flammability test) with a 5 wt% EG content, whereas 10 wt% EG was adequate for a lowered rate of combustion, as observed from cone calorimetry. Mu *et al*. [32] reported improved thermal stability, flame retardancy, synergistic effect and anti-dripping performance of melt-blended PLA/EG/poly(bis(phenoxy) phosphazene) composites. This was attributed to the combined effect of the gas and condensed phase flame retardant mechanism of EG and the phosphazene polymer. Zhu *et al*. [33] observed a synergistic effect of EG/ammonium polyphosphate (APP) (1:3) at 15 wt% in melt-blended PLA composites and attributed it to the formation of compact, dense and stable char protection layers that resulted from the filling of gaps between EG flakes with the viscous decomposition products from APP/PLA.

The aim of the study reported in this article was to investigate the thermal degradation and combustion properties of Cereplast PLA (PLA-starch blend), loaded with commercial grade expandable graphite (EG). This was achieved by melt compounding PLA-starch with EG at 5, 10 and 15 wt% loadings and characterizing the PLA-starch/EG composites for their thermal stability, evolved volatile pyrolysis products and flammability performance. This investigation is

the basis of a series of studies on the use of a commercial expandable graphite grade as a halogen-free flame retardant for biopolymers and their blends.

2 MATERIALS AND METHODS

2.1 Materials

Polylactic acid (PLA-starch blend) is a sustainable 1001 injection molding grade, containing additives derived from starch and other renewable resources, with physical properties as shown in Table 1. The commercial expandable graphite (EG) used was an ES250 B5 grade, consisting of 90–95% carbon content, expansion rate of 250–500 cm^3 g^{-1} at a starting temperature range of between 180–300 °C, and a particle size of 80% (of the particles) > 300 µm supplied by Qingdao Kropfmuehl Graphite, China. It contained $KMnO_4$ as an oxidant and H_2SO_4 as an intercalant [23, 34]. The materials were used as received from the suppliers without any modification/purification, except for drying at 50 °C prior to the compounding.

2.2 Sample Preparation

The samples were compounded (according to the ratios shown in Table 2) after drying overnight and were prepared by melt-mixing, using a Brabender Plastograph with a mixing volume of 55 cm^3. The mixing temperature was 180 °C at a rotational speed of 60 rpm for 12 minutes. This was followed by hot melt-pressing at the temperature of 180 °C under 50 bar for 5 min in order to obtain 140 × 140 × 2 mm square sheets.

2.3 Sample Analysis

The TGA analyses were carried out in a PerkinElmer STA 6000 simultaneous thermal analyzer. The samples (mass range 20–25 mg) were heated from 30 to 700 °C, at a heating rate of 10 °C min^{-1} under flowing nitrogen (flow rate 20 mL min^{-1}). In this study, the TGA technique was mainly employed to examine the thermal stability and char content of the samples.

The thermal decomposition volatiles of the samples were analyzed using the TGA connected to a PerkinElmer Spectrum 100 Fourier transform infrared spectrometer (TGA-FTIR). The same temperature range and heating rate were used as in the case of TGA analysis and the volatiles were transferred to the FTIR by a PerkinElmer TL 8000 balanced flow FTIR EGA system. The spectra were collected continuously during the degradation process.

The flammability tests were performed using a cone calorimeter (FTT, UK) according to ISO 5660-1 at a heat flux of 35 kW m^{-2}. The samples had dimensions of 100 mm × 100 mm × 2 mm and were prepared by compression molding. The samples were wrapped with an aluminium foil on the sides and at the bottom and placed in a retainer frame over low density ceramic wool and then secured on the specimen holder. The following quantities were measured using the cone calorimeter: heat release rate, time to ignition, mass loss rate, as well as carbon monoxide and carbon dioxide yields.

In order to determine the morphology of the char residues after combustion in the cone calorimeter,

Table 2 Sample compositions of the PLA-starch/EG composites.

Sample	Composition [wt. %]
PLA-starch	100
PLA-starch/EG-5	95/5
PLA-starch/EG-10	90/10
PLA-starch/EG-15	85/15

Table 1 Physical properties of PLA-starch blend, Cereplast Sustainable Resin 1001 grade [45].

Physical property	ASTM test method	Values
Tensile strength at maximum	D 638	49.6 MPa
Tensile elongation at break	D 638	5.1%
Tensile modulus	D 638	3,590 MPa
Flexural modulus	D 790	3,360 MPa
Flexural strength	D 790	80 MPa
Gardner impact	D 5420	1.13 J
Notched Izod impact strength (at 23 °C)	D 256	40 J m^{-1}
Temperature deflection under 0.45 MPa	D 648	44 °C
Melt flow index 190 °C at 2.16 kg	D 1238	8 g/10 min
Density	D 792 Method A	1.28 g ml^{-1}

an FEI Quanta 200 environmental scanning electron microscope (ESEM) was used and the analyses were done at room temperature. The samples were gold-coated by sputtering in order to obtain conductive coatings on the samples.

3 RESULTS AND DISCUSSION

3.1 Thermogravimetric Analysis (TGA)

The TGA and DTG results of the PLA-starch/EG composites are shown in Figure 1 and the related data are summarized in Table 3. $T_{2\%}$ and $T_{60\%}$ represent the mass loss temperatures at 2 and 60 wt% mass loss, respectively, while T_{max} is the temperature at maximum degradation rate. The $T_{2\%}$ is normally considered as the onset temperature of thermal degradation. The char residue % for the composites at 700 °C is also reported.

From Figure 1a it is observed that PLA-starch blend degrades in two steps and leaves some residues. The first step occurs over the temperature range 270–337 °C and its T_{max} is 321 °C. This step is due to the thermal degradation of PLA component. The thermal degradation of PLA is reported to be a complex process, involving several reaction mechanisms with at least one dominating [35]. The reaction mechanisms may include non-radical and radical reactions, viz., i) random chain scission, ii) depolymerization, iii) thermo-oxidative degradation, iv) intramolecular and intermolecular transesterifications, v) hydrolytic degradation, vi) pyrolytic elimination and vii) radical reactions. It is, however, considered that the main thermal degradation mechanism for PLA is due to intramolecular transesterification reactions [36]. In addition, there is a simultaneous recombination of the cyclic oligomers that were formed with linear polyesters through insertion reactions [35]. This led to the formation of cyclic oligomers of lactic acid and lactide. Other thermal decomposition products of PLA reported in the literature include carbon monoxide and carbon dioxide, acetaldehyde (i.e., believed to

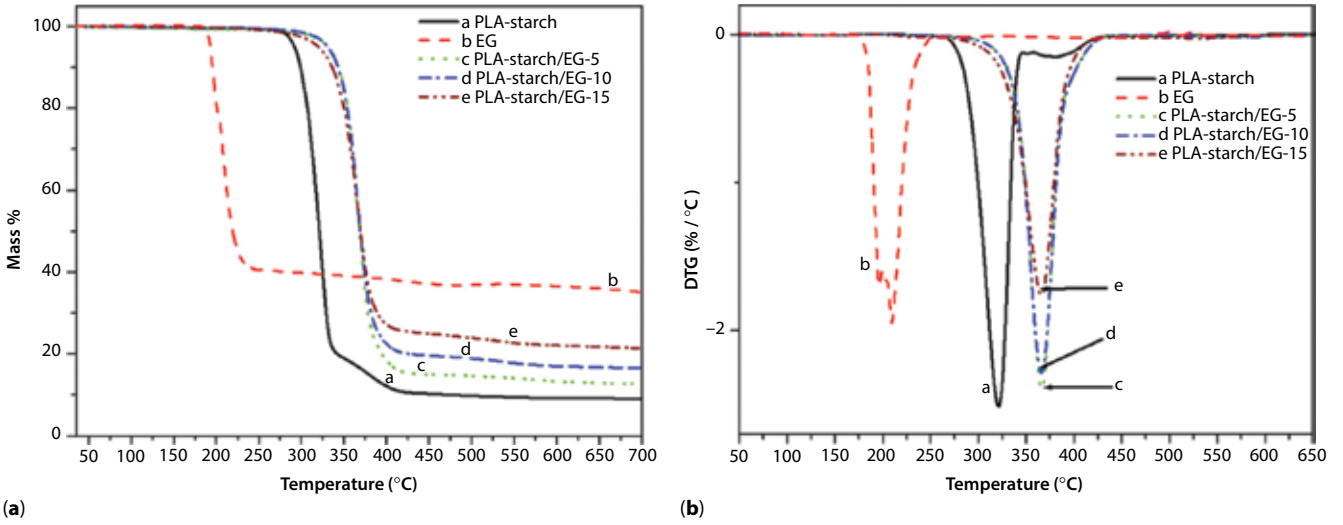

Figure 1 (**a**) TGA and (**b**) DTG curves of PLA-starch/EG composites.

Table 3 TGA results of investigated PLA-starch/EG composite materials.

Sample	$T_{2\%}$ [°C]	$T_{60\%}$ [°C]	T_{max} [°C]	Residue at 70 °C [%]
PLA-starch	282	325	321 & 381	9.1
EG	190	–	196 & 209	35
PLA-starch/EG-5	306	372	368	12.7 (14)
PLA-starch/EG-10	310	374	374	16.4 (18)
PLA-starch/EG-15	291	376	376	21.2 (23)

$T_{2\%}$ and $T_{60\%}$, temperatures at 2 and 60% weight loss, respectively; T_{max}, temperature at maximum mass loss rate from DTG. The values in parenthesis are the expected residue % (at 700 °C) calculated from: {residue % of PLA (e.g., 9.1%) × weight fraction of the blend (e.g., 0.95) + weight fraction of EG (e.g., 5%) = 14%}.

decompose into methane and butanedione), methyleketene and water [37]. The second thermal degradation step occurs between 337 and 460 °C with T_{max} of 381 °C. This is due to the degradation of the char from the starch and other renewable resources-based additives in PLA-starch blend. The thermal degradation of PLA-starch yielded a char residue of about 9.1% at 700 °C, which is attributable to the presence of starch and other renewable resource additives in PLA-starch blend [38]. Likewise, EG degrades via a two-step process with a maximum decomposition temperature of 209 °C. This relates to the exfoliation process of the expandable graphite starting at around 190 °C, due to the escape of SO_2 and CO_2 inert gases [16, 22, 23].

All the PLA-starch/EG composites decompose in one major step, occurring over a temperature range of 258–420 °C (Figures 1a,b). It is observed that the incorporation of EG microparticles in PLA-starch blend shifts the thermal degradation curves to higher temperatures (Table 3). This is attributed to the good barrier effect of the graphite micro-sheets due to swelling [30, 39]. It seems that this step has overlapped with the second degradation step observed for PLA-starch, since they occur within a similar temperature range. The onset temperature of thermal decomposition ($T_{2\%}$) is higher for the composites when compared with the PLA-starch (Table 3), but the increase is inconsistent with EG loadings. The PLA-starch/EG-10 composition recorded the highest value of 310 °C, whereas the PLA-starch/EG-15 yielded the lowest of the composites (i.e., 291 °C). This may be attributed to i) the quick degradation of EG since the reaction between H_2SO_4 and graphite produces blowing gases above 190 °C and ii) high thermal conductivity of EG [30, 33]. Similar findings were reported by Zhu *et al*. [33], who investigated the synergistic effect between expandable graphite and ammonium polyphosphate on flame-retarded PLA. Furthermore, $T_{60\%}$ and T_{max} increased with EG loadings. This is attributable to the presence of EG, which improved the thermal stability of the PLA-starch/EG composites. The char residue of the composites is higher than that of neat PLA-starch. However, the experimentally observed % residue is less than the calculated % residue (Table 3: values in parentheses). This is probably due to thermal degradation reaction(s) that are not in favor of yielding carbon, instead proceeding by the formation of CO and CO_2 volatile gases. From the TGA results it can be seen that the presence of EG improved the thermal stability of PLA-starch/EG composites.

3.2 Volatile Products of PLA-starch and PLA-starch/EG Composites: TGA-FTIR Analysis

The FTIR spectra of PLA-starch and the PLA-starch/EG composites at temperatures where the maximum pyrolysis products were given off are illustrated in Figure 2. It is observed that there are different

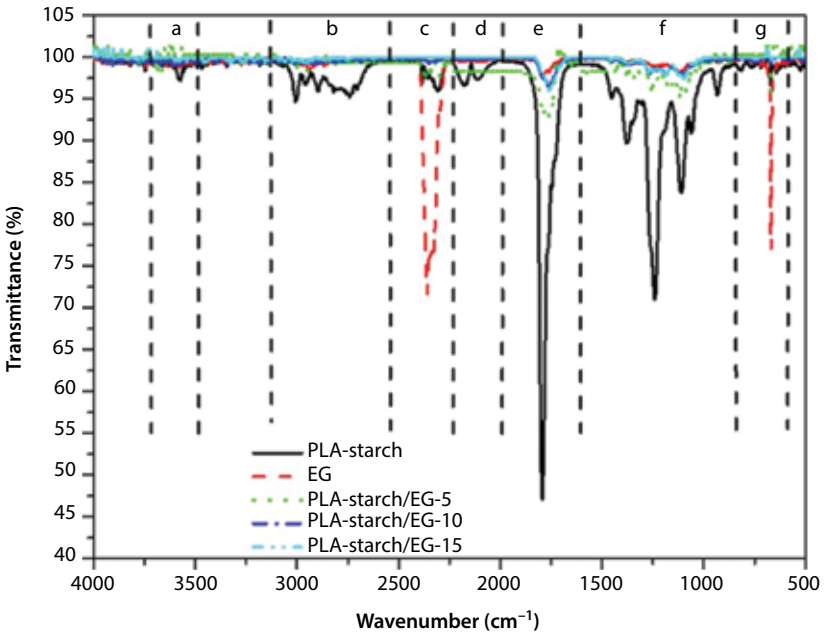

Figure 2 FTIR spectra of the PLA-starch/EG composites at the temperatures where the maximum pyrolysis products were given off.

absorption regions labeled a to g, consisting of ranges of wavenumbers; a: 3747–3573 cm^{-1}, b: 3008–2500 cm^{-1}, c: 2500–2300 cm^{-1}, d: 2300–2000 cm^{-1}, e: 2000–1700 cm^{-1}, f: 1500–900 cm^{-1} and g: 900–600 cm^{-1}. From this, it may be inferred that the main pyrolysis products are made up of compounds that contain –OH groups (regions a and f), C–H (hydrocarbons, $–CH_3$ and $–CH_2$ groups, both stretching and bending modes) (region b), CO_2 (regions c & g), CO (region d); carbonyl (C=O) containing groups (region e) and aliphatic esters (C–O–C) and C–O stretch (region f) [40–42]. It can be observed that EG exhibits absorption spectra at regions c, e, f and g, indicating the evolution of CO_2, C–O and carbonyl-containing compounds (C=O), as well as water- or acid (–OH)-based groups. The bands associated with CO_2 (regions c and g) are strong for EG, showing that EG produces more carbon dioxide gas. On the other hand, PLA-starch blend exhibits characteristic absorption bands in most of the regions, except at g. This indicates that the pyrolysis products of PLA-starch are possibly water, aldehydes, CO_2 and CO, and aliphatic esters.

For the PLA-starch/EG composites, it is observed that there are fewer pyrolysis products when compared with those of PLA-starch and EG alone. The incorporation of EG into PLA-starch (i.e., 5 wt% EG) resulted in less intense absorption bands in all the regions. However, at higher EG contents (i.e., 10 and 15 wt%), only the regions (e and f) associated with carbonyl and aliphatic ester groups, respectively, are observed. This indicates that EG is effective at hindering the formation and evolution of pyrolysis products of the PLA-starch/EG composites.

3.3 Cone Calorimetry

The cone calorimetric results of the PLA-starch/EG composites are shown in Figures 3 to 6 and the data are summarized in Tables 4 and 5. The fire performance index (FPI) was calculated according to Equation 1 [43].

$$FPI = \frac{TTI}{PHRR} \quad (1)$$

It can be seen that the incorporation of EG into PLA-starch blend reduces the time to ignition (TTI) of the composites (Table 4). The reduction is nonetheless inconsistent with the EG content. The TTI is lowered from 44 s for PLA-starch blend to 31 s for the PLA-starch/EG-5 composite. The lower TTI is attributed to the low thermal stability and quick decomposition of EG, occurring at a lower temperature (i.e., 190 °C, as seen from the TGA results in Section 3.1) than for PLA-starch blend (i.e., onset temperature of decomposition is 282 °C) [44]. In this case, sufficient quantities of flammable volatile(s) (i.e., acetaldehyde which decomposes into methane and butanedione) were released at an earlier stage in order to initiate ignition. Similar findings were reported by Focke *et al*. [22], who observed a decrease in TTI from ~58 s for low-density polyethylene (LDPE) to ~46 s for 10 wt% EG filled LDPE.

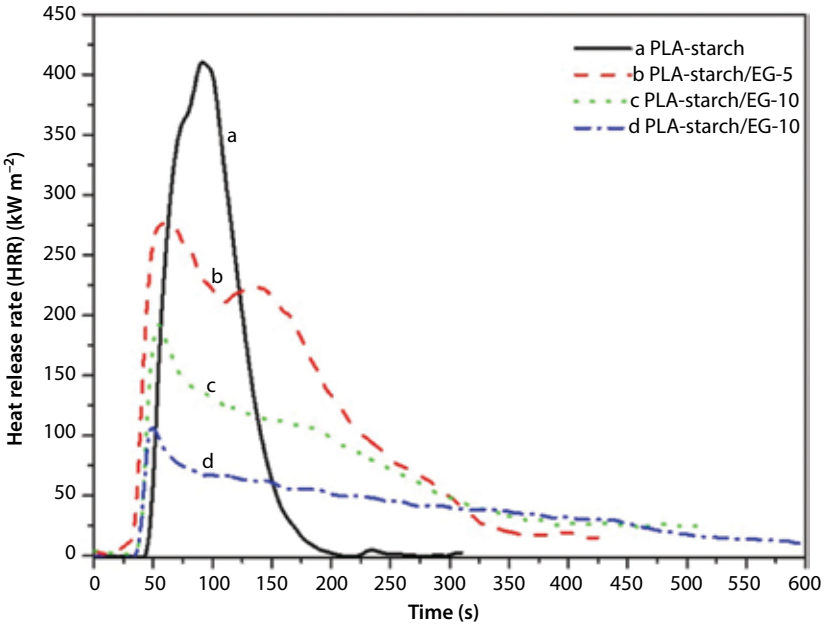

Figure 3 Heat release rate (HRR) curves for PLA-starch and PLA/EG composites at various EG contents.

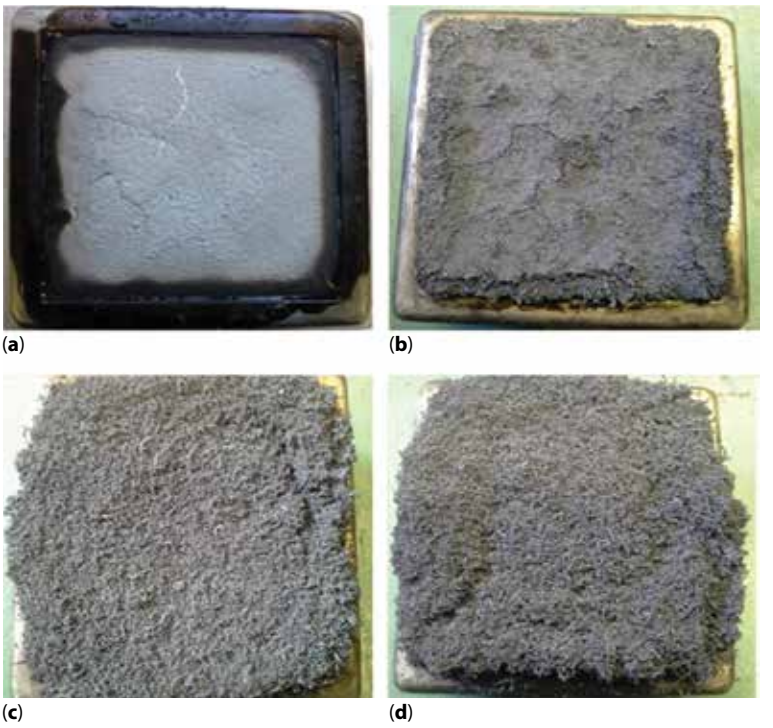

Figure 4 Images of ash samples after cone calorimetry tests of (**a**) PLA-starch; and PLAstarch/EG composites at (**b**) 5, (**c**) 10 and (**d**) 15 wt% EG.

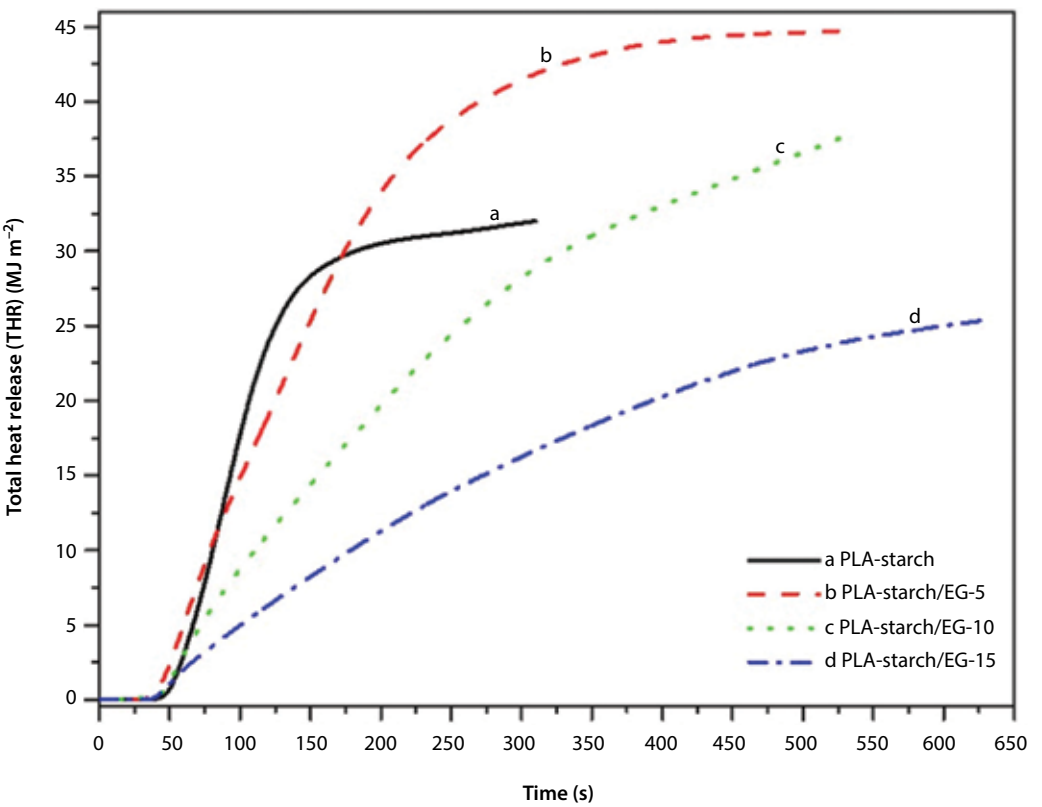

Figure 5 Total heat release (THR) curves of PLA-starch and PLA-starch/EG composites.

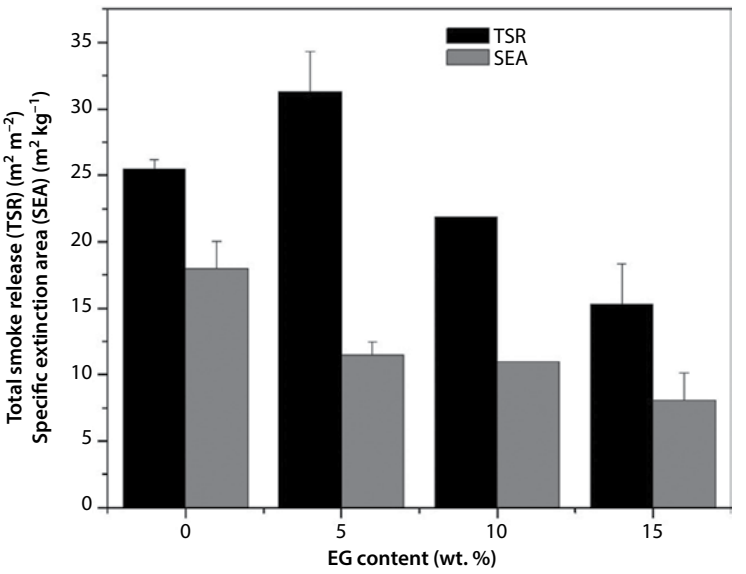

Figure 6 Total smoke release (TSR) and specific extinction area (SEA) versus EG content.

Table 4 Cone calorimetric results (at 35 kW m-2 heat flux) of all the investigated samples.

Parameter	PLA-starch	PLA-starch/EG-5	PLA-starch/EG-10	PLA-starch/EG-15
TTI [s]	44 ± 0	31 ± 0.9	35 ± 1	33 ± 1
PHRR [kW m^{-2}]	363 ± 0 414 ± 0	276 ± 2 224 ± 2	194 ± 4	109 ± 5
THR [MJ m^{-2}]	30 ± 2	45 ± 1	36 ± 2	26 ± 3
EHC [MJ kg^{-2}]	16 ± 0	18 ± 1	20 ± 0	17 ± 2
av-MLR [gs^{-1} m^{-2}]	8.6 ± 0.3	8.9 ± 0.6	4.7 ± 0.3	2.9 ± 0.0
MARHE [kW m^{-2}]	199 ± 6	175 ± 3	100 ± 2	58 ± 4
FPI [kW m^{-2}s^{-1}]	0.11	0.11	0.18	0.30

TTI, time to ignition; PHRR, peak heat release rate; THR, total heat release; EHC, effective heat of combustion; av-MLR, average mass loss rate; MARHE, maximum average rate of heat emission; and FPI, fire performance index.

The dynamic curves of heat release rate (HRR) for PLA-starch blend in Figure 3 show the characteristic shape of a thermally thin sample [22]. Thermally thin samples are characterized by sharp peak HRR curves when the whole sample is pyrolyzed at once. The HRR curves for thermally thick, char-forming samples, exhibit a sudden rise to a plateau value [22] and this phenomenon is observed in flame-retarded samples. The HRR is clearly lowered for the PLA-starch/EG composites with respect to the PLA-starch matrix. It is observed that PLA-starch blend shows a peak shoulder at 363 kW m^{-2} (i.e., at 75 s), which is related to the starch component, whereas the maximum peak at 414 kW m^{-2} (i.e., at 90 s) relates to PLA component. Likewise, the PLA-starch/EG-5 composite shows two clearly defined peaks at 276 (i.e., at 60 s) and 224 kW m^{-2} (i.e., at 130 s). The peak heat release rate (PHRR) values, as a function of EG content of the composites, decreased from 414 kW m^{-2} for PLA-starch blend to 109 kW m^{-2} (Table 4). This shows a reduction of 33, 53 and 74% for the 5, 10 and 15 wt% EG contents, respectively. The improved fire performance with respect to PHRR is due to the formation of an insulating protective intumescent char barrier at the solid surface of the composites. This is shown in Figure 4, where the exfoliated intumescent graphite char layer was formed consistently with EG loadings. This formed a barrier that has limited the transfer of heat from the source to the substrate and consequently slowed down the thermal degradation of the composites, thus minimizing the rate at which flammable volatiles are evolved [16, 22]. This is further confirmed by the average mass loss rate (av-MLR) data in Table 4, whereby a reduction is observed from 8.9 g s^{-1} m^{-2} for PLA-starch blend

Table 5 Smoke emission parameters of neat PLA-starch and the PLA-starch/EG composites from cone calorimetry (35 kW m^{-2} heat flux).

Parameter	PLA-starch	PLA-starch/EG-5	PLA-starch/EG-10	PLA-starch/EG-15
TSR [m^2 m^{-2}]	25.5 ± 0.7	31.3 ± 3.0	21.9 ± 0.0	15.3 ± 3.0
SEA [m^2 kg^{-1}]	18 ± 2	11.5 ± 1.0	11 ± 0	8.1 ± 2.0
CO (×10^{-3}) [kg kg^{-1}]	13 ± 0	41.7 ± 5.0	89.4 ± 1.0	119 ± 1
CO_2 [kg kg^{-1}]	1.3 ± 0.0	1.6 ± 0.0	1.4 ± 0.0	1.3 ± 0.0
CO/CO_2 (×10^{-3})	10	26.1	63.9	91.4

to 2.9 g s^{-1} m^{-2} for the PLA-starch/EG-15 composite, although the 5 wt% EG sample proves to be different. Furthermore, the exfoliation of EG is an endothermic process with the attendant consequence of lowering the temperature of the medium, manifesting in a cooling effect of a physical mode of action. The reduction in PHRR is also attributed to a dilution effect of the CO_2 and H_2O, produced during the exfoliation of the EG in the composites [17, 44].

As shown in Figure 4 for the samples after combustion using the cone calorimeter, PLA-starch blend left a grey powdery ash with some oily-like molten material on the edges of the retainer frame (Figure 4a). In the presence of 5 wt% EG, a cracked and very lightly covered surface composed of grey ash and carbonaceous exfoliated graphite is observed (Figure 4b). The ash is limited within the frame. At high EG contents (i.e., 10 and 15 wt%), it is observed that the ash content is high and it even overflowed beyond the retainer frame. As discussed in the introduction, the entire process described for the exfoliation of EG played a key role in lowering the temperature of the medium, diluting the evolved flammable volatile gases by producing inert gases and forming a barrier of carbonaceous exfoliated graphite. These have aided in improving the flammability performance of the PLA-starch/EG composites.

Figure 5 and Table 4 illustrate the total heat release (THR) of PLA-starch blend and the PLA-starch/EG composites. The slope of the THR curve is assumed to be representative of the flame spread rate [44]. It is observed that PLA-starch blend showed a higher flame spread (i.e., steeper slope) with a THR value of 30 MJ m^{-2}. The incorporation of EG at 5 and 10 wt% into PLA-starch, respectively led to 33 and 17% increases in THR compared to PLA-starch blend. It can be seen that the flame spread rates of the PLA-starch/EG composites (especially at 10 and 15 wt% EG loadings) were less than that of PLA-starch blend. A decrease in THR to 26 MJ m^{-2}, corresponding to a 17% reduction, was observed for the 15 wt% EG composite. The results indicate that the composite, at the highest EG loading, is partially protected by the exfoliated EG without complete combustion. At 5 and 10 wt% EG loadings, however, it seems that the barrier is insufficient to prevent the release of volatile combustion products [5]. Furthermore, from Table 4 it can be seen that the effective heat of combustion (EHC) is high for all the composites (i.e., around 17–20 MJ kg^{-1}) when compared to that of PLA-starch blend (i.e., 16 MJ kg^{-1}). This indicates that the carbon and hydrogen atoms in the composite samples can easily react with oxygen in air to produce carbon dioxide and water and hence release a large amount of heat during combustion [19, 20]. It is also observed (Table 4) that the average mass loss rate (av-MLR) increased by 3% at 5 wt% EG content, then decreased by 45 and 66% at 10 and 15 wt% EG loadings, respectively, with respect to PLA-starch blend. The slight increase in av-MLR is attributed to the catalytic effect of EG on the combustion of PLA-starch/EG composites since sufficient quantities of flammable volatiles were released at an earlier stage at this content. The reduced av-MLR at high EG loadings is due to the effect of EG that slowed down the rate of mass loss of PLA-starch/EG composites leading to incomplete combustion (see smoke emission behavior discussion on CO/CO_2 ratio).

The maximum average rate of heat emission (MARHE) and fire performance index (FPI) are also reported in Table 4. The MARHE parameter provides a measure of the inclination for fire development under real scale conditions [22]. Generally, it can be seen that the MARHE is reduced with the incorporation of EG, i.e., from 199 kW m^{-2} for PLA-starch to 58 kW m^{-2} at the highest EG content. It corresponds to 12, 50 and 71% reduction in MARHE at 5, 10 and 15 wt% EG levels, respectively. This indicates that the PLA-starch/EG composites have less tendency for fire development under real scale conditions. The FPI parameter further provides for the estimation of the predicted fire spread rate and size of a real fire. It is considered a good indicator of the contribution of fire growth of materials [43]. The results show no change in the FPI value for the 5 wt% EG containing sample, while a reduction of 39 and 63% in FPI was observed for the 10 and 15 wt%

EG containing samples, respectively. It is concluded that the PLA-starch/EG composites at high EG loadings (i.e., 10 and 15 wt%) have little contribution to fire growth in a real fire situation.

Table 5 and Figure 6 show that the smoke emission behavior in terms of TSR and SEA were improved in the presence of EG. The TSR at 5 wt% EG loading was increased by 19%. This is attributed to EG that may have prevented the combustion of the gas containing fragments of the decomposed PLA-starch matrix with subsequent incomplete burning of these decomposed fragments, thus resulting in higher concentration of smoke [29]. However, the TSR was reduced by 14 and 40% at 10 and 15 wt% EG contents, respectively. The SEA, which signifies the smoke density, was lowered by 36, 39 and 55% at 5, 10 and 15 wt% EG loadings, respectively. The improvements in TSR and SEA parameters indicate that EG acted as a smoke suppressant in the PLA-starch/EG composites, especially at increased filler contents (i.e., 10 and 15 wt% EG). The composites exhibited high CO yields as a function of EG content when compared to PLA-starch blend. This is related to the presence of EG due to the high level of oxidation during its manufacturing, which when heated above ~200 °C, produces carbon monoxide as one of the products [16]. Likewise, the CO_2 yield was high in the presence of EG, but comparable to that of PLA-starch at the highest EG content. The CO/CO_2 ratio (Table 5) increased as a function of EG loading. This signifies the incomplete combustion of the composites in the presence of the EG microfiller.

In order to further clarify the flame retardancy mechanism of the PLA-starch/EG composites, the morphology and structure of the char residues of the composites after combustion were investigated by ESEM. As shown in Figure 7, an exfoliated structure of the residues with embedded microspheres is observed for all the composites investigated after cone calorimetry tests. A weak, short and lighter char structure with numerous holes is seen for the 5 wt% EG containing composite (Figure 7a,d). The presence of holes is believed to originate from the blowing gases in the redox reaction between residual H_2SO_4 and the graphite, according to Reaction Equation 2 [25]. The surface is covered by grey ash (as seen from Figure 4), owing to a large quantity of polymeric material when compared to EG content. Since there

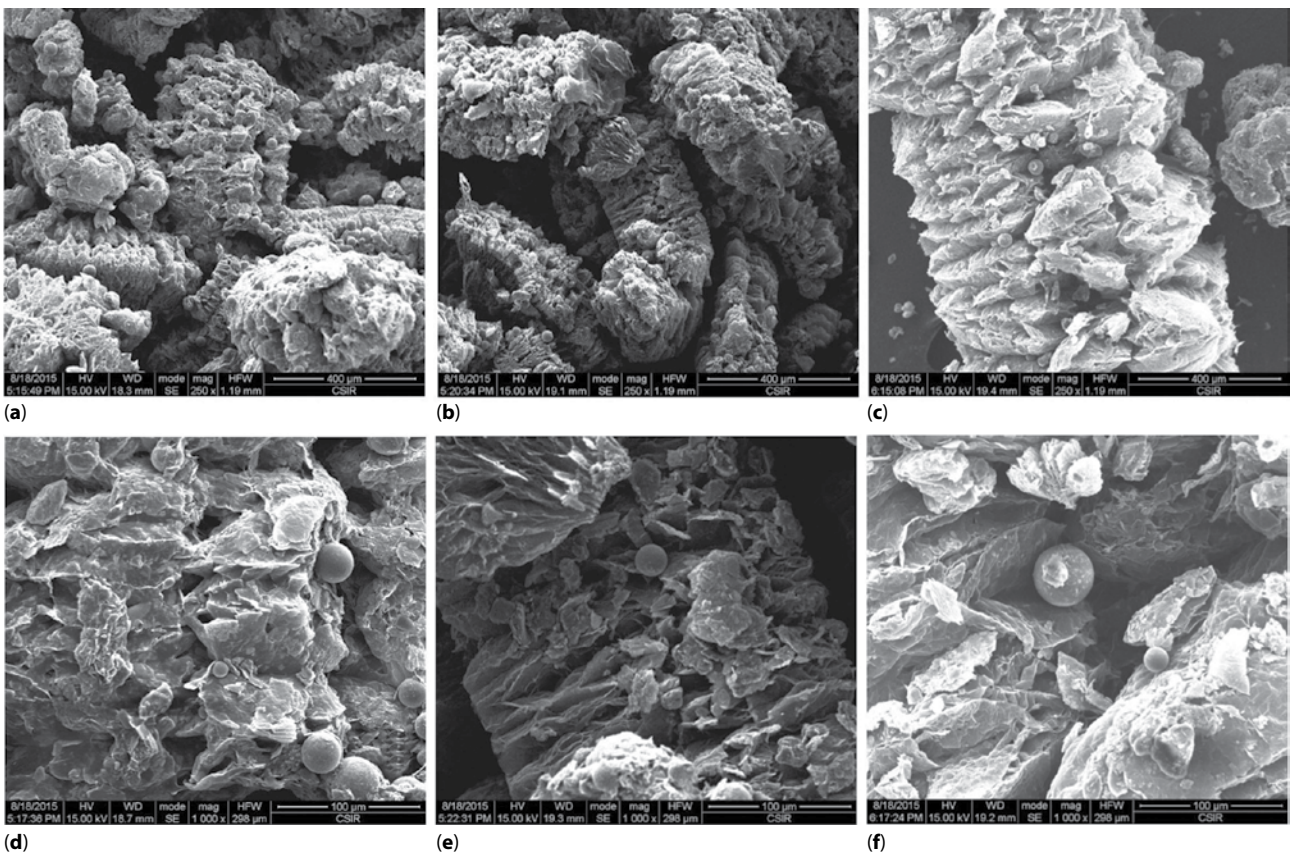

Figure 7 SEM micrographs of the char residues after combustion in the cone calorimeter: (**a**,**d**) PLA-starch/EG-5; (**b**,**e**) PLA-starch/EG-10, and (**c**,**f**) PLA starch/EG-15.

was some level of incomplete combustion (i.e., 62%, Table 5), this observation is due to char residue from starch and other renewable resource materials and the silicon-based materials (i.e., glass) [38] present in PLA-starch blend. There is a fairly long, brittle and continuous exfoliated char structure, the surface of which has some pocket-like structures, for the 10 wt% EG composite (Figure 7b,e). A thick and strong worm-like structure is observed for the 15 wt% EG content composite (Figure 7c,f). This formed an effective protective char layer that accounts for the improved fire resistance performance, as observed from the cone calorimetry results.

$$C + 2H_2SO_4 \rightarrow CO_2 + 2SO_2 + 2H_2O \qquad (2)$$

4 CONCLUSIONS

Poly(lactic acid)-starch/expandable graphite (PLA-starch/EG) flame retardant composites were prepared and their thermal degradation stability, volatile pyrolysis products and flammability properties were studied. EG microfiller increased the $T_{2\%}$, $T_{60\%}$ and T_{max} due to the shielding effect of EG, thereby improving the thermal degradation stability of the PLA-starch/EG composites. Although the char content increased with filler loading, the experimental % char content of the composites was less than the sum of the % residue from PLA-starch and the wt% EG initially mixed with PLA-starch blend. The flammability performance of the PLA-starch/EG composites was improved, especially at 15 wt% EG content. The PHRR, TSP and SEA were reduced significantly by 74, 40 and 55% reduction compared to PLA-starch blend, respectively. This was due to the key property and ability of EG to exfoliate at elevated temperatures, during which time three effects (i.e., via physical mode of action) were in place: i) cooling effect, ii) dilution effect and iii) the formation of an effective protective intumescent char layer that prevented heat transfer from the source to the composite substrates, and mass transfer from the composite to the flame zone were experienced. This has further excluded the oxygen necessary for combustion. However, since the combustion of EG resulted in CO, CO_2 and heat, the composites were characterized by high CO and CO_2 yields, as well as high THR and EHC. Further work is underway to find some alternative ways of improving these above shortfalls.

ACKNOWLEDGMENTS

The financial assistance of the National Research Foundation for this research is hereby acknowledged. Opinions expressed and conclusions arrived at are those of the authors and are not necessarily to be attributed to the NRF. Acknowledgment is also extended to colleagues and researchers for their undivided attention and support.

REFERENCES

1. D. Garlotta, A literature review of poly(lactic acid). *J. Polym. Environ.* **9**(2), 63–83 (2001).
2. A.P. Gupta and V. Kumar, New emerging trends in synthetic biodegradable polymers – Polylactide: A critique. *Eur. Polym. J.* **43**, 4053–4074 (2007).
3. R.M. Rasal, A.V. Janorkar, and D.E. Hirt, Poly(lactic acid) modifications. *Prog. Polym. Sci.* **35**, 338–356 (2010).
4. S. Saeidlou, M.A. Huneault, H. Li, and C.B. Park, Poly(lactic acid) crystallization. *Prog Polym. Sci.* **37**, 1657–1677 (2012).
5. P. Wei, S. Bocchini, and G. Camino, Flame retardant and thermal behavior of polylactide/expandable graphite composites. *Polimery.* **58**(5), 361–364 (2013).
6. K. Fukushima, M. Murariu, G. Camino, and P. Dubois, Effect of expanded graphite/layered-silicate clay on thermal, mechanical and fire retardant properties of poly(lactic acid). *Polym. Degrad. Stab.* **95**, 1063–1076 (2010).
7. G. Huang, J. Gao, X. Wang, H. Liang, and C. Ge, How can graphene reduce the flammability of polymer nanocomposites?. *Mater. Lett.* **66**,187–189 (2012).
8. M.E. Mngomezulu, M.J. John, V. Jacobs, and A.S. Luyt, Review on flammability of biofibres and biocomposites. *Carbohyd. Polym.* **111**, 149–182 (2014). DOI: 10.1016/j.carbpol.2014.03.071
9. M. Murariu, A.L. Dechief, L. Bonnaud, Y. Paint, A. Gallos, G. Fontaine, S. Bourbigot, and P. Dubois, The production and properties of polylactide composites filled with expanded graphite. *Polym. Degrad. Stab.* **95**, 889–900 (2010).
10. C. Vogel and H.W. Siesler, Thermal degradation of poly(ε-caprolactone), poly(L-lactic acid) and their blends with poly(3-hydroxy-butyrate) studies by TGA/FT-IR spectroscopy. *Macromol. Symp.* **265**, 183–194 (2008).
11. D. Wu, Y. Zhang, M. Zhang, and W. Zhou, Phase behaviour and its viscoelastic response of polylactide/poly(ε-caprolactone) blend. *Eur. Polym. J.* **44**, 2171–2183 (2008).
12. G. Bai, C. Guo, and L. Li, Synergistic effect of intumescent flame retardant and expandable graphite on mechanical and flame-retardant properties of wood flour-polypropylene composites. *Constr. Build. Mater.* **50**, 148–153 (2014).
13. J.D. Lee, *Concise Inorganic Chemistry*, pp. 402–420, Chapman & Hall Ltd., Singapore (1995).
14. R. Sengupta, M. Bhattacharya, S. Bandyopadhyay, and A.K. Bhowmick, A review on the mechanical and electrical properties of graphite and modified graphite reinforced composites. *Prog. Polym. Sci.* **36**, 638–670 (2011).
15. E.D. Weil and S.V. Levchik, Flame retardants in commercial use or development for polyolefins. *J. Fire Sci.* **26**, 5–43 (2008).

16. W.W. Focke, H. Badenhorst, W. Mhike, H.J. Kruger, and D. Lombaard, Characterization of commercial expandable graphite fire retardants. *Thermochim. Acta.* **584**, 8–16 (2014).
17. Z. Wang, E. Han, and W. Ke, Influence of expandable graphite on fire resistance and water resistance of flame-retardant coatings. *Corros. Sci.* **49**, 2237–2253 (2007). DOI: 10.1016/j.corsci.2006.10.024
18. S. Bourbigot, and G. Fontaine, Flame retardancy of polylactide: An overview. *Polym. Chem.* **1**, 1413–1422 (2010).
19. R. Xie and B. Qu, Synergistic effects of expandable graphite with some halogen-free flame retardants in polyolefin blends. *Polym. Degrad. Stab.* **71**, 375–380 (2001).
20. R. Xie and B. Qu, Thermo-oxidative degradation behaviours of expandable graphite-based intumescent halogen-free flame retardant LLDPE blends. *Polym. Degrad. Stab.* **71**, 395–402 (2001).
21. W. Mhike, W.W. Focke, J.P. Mofokeng, and A.S. Luyt, Thermally conductive phase-change materials for energy storage based on low-density polyethylene, soft Fischer-Tropsch wax and graphite. *Thermochim. Acta.* **527**, 75–82 (2012).
22. W.W. Focke, H.J. Kruger, W. Mhike, A. Taute, A. Roberson, and O. Ofosu, Polyethyelene flame retarded with expandable graphite and a novel intumescent additive. *J. Appl. Polym. Sci.* **40493**, 1–8 (2014).
23. W.W. Focke, H. Muiambo, W. Mhike, H.J. Kruger, and O. Ofosu, Flexible PVC flame retarded with expandable graphite. *Polym. Degrad. Stab.* **100**, 63–69 (2014).
24. F.M. Uhl, Q. Yao, H. Nakajima, E. Manias, and C.A. Wilkie, Expandable graphite/polyamide-6 nanocomposites. *Polym. Degrad. Stab.* **89**, 70–84 (2005).
25. X.-Y. Pang and M.-Q. Weng, Preparation of expandable graphite composite under the auxiliary intercalation of zinc sulfate and its flame retardancy for ethylene/vinyl acetate copolymer. *Int. J. ChemTech Res.* **6**(2), 1291–1298 (2014).
26. L. Gao, G. Zheng, Y. Zhou, L. Hu, G. Feng, and Y. Xie, Synergistic effect of expandable graphite, melamine polyphosphate and layered double hydroxide on improving the fire behavior of rosin-based rigid polyurethane foam. *Ind. Crop. Prod.* **50**, 638–647 (2013).
27. L. Gao, G. Zheng, Y. Zhou, L. Hu, G. Feng, and M. Zhang, Synergistic effect of expandable graphite, diethyl ethylphosphonate and organically-modified layered double hydroxide on flame retardancy and fire behavior of polyisocyanurate-polyurethane foam nanocomposite. *Polym. Degrad. Stab.* **101**, 92–101 (2014).
28. L. Qian, F. Feng, and S. Tang, Bi-phase flame-retardant effect of hexa-phenoxy-cyclotriphosphazene on rigid polyurethane foams containing expandable graphite. *Polymer* **55**, 95–101 (2014).
29. F. Feng and L. Qiang, The flame retardant behaviors and synergistic effect of expandable graphite and dimethyl methylphosphonate in rigid polyurethane foams. *Polym. Compo.* **35**, 301–309 (2014).
30. J. Liu, Y. Zhang, S. Peng, B. Pan, C. Lu, H. Liu, J. Ma, and Q. Niu, Fire property and charring behaviour of high impact polystyrene containing expandable graphite and microencapsulated red phosphorus. *Polym. Degrad. Stab.* **121**, 261–270 (2015).
31. S. Yang, J. Wang, S. Huo, M. Wang, J. Wang, and B. Zhang, Synergistic flame-retardant effect of expandable graphite and phosphorus-containing compounds for epoxy resin: Strong bonding of different carbon residues. *Polym. Degrad. Stab.* **128**, 89–98 (2016).
32. X. Mu, B. Yuan, W. Hu, S. Qiu, L. Song, and Y. Hu, Flame retardant and anti-dripping properties of polylactic acid/poly(bis(phenoxy)phosphazene)/expandable graphite composite and its flame retardant mechanism. *RSC Adv.* **5**, 76068–76078 (2015).
33. H. Zhu, Q. Zhu, J. Li, K. Tao, L. Xue, and Q. Yan, Synergistic effect between expandable graphite and ammonium polyphosphate on flame retarded polylactide. *Polym. Degrad. Stab.* **96**, 183–189 (2011).
34. Qingdao Kropfmuehl Graphite Co., Ltd., http://www.gk-graphite.cn/fileadmin/user_upload/PDF/List_standard.pdf (26 October 2015).
35. F. Carrasco, P. Pagès, J. Gámez-Pérez, O.O. Santana, and M.L. Maspoch, Processing of poly(lactic acid): Characterization of chemical structure, thermal stability and mechanical properties. *Polym. Degrad. Stab.* **95**, 116–125 (2010).
36. C.A. Nicolae, M.A. Grigorescu, and R.A. Gabor, An investigation of thermal degradation of poly(lactic acid). *Eng. Lett.* **16**(4), 568, EL_16_4_16 (2008).
37. F.D. Kopinke, M. Remmler, K. Mackenzie, M. Milder, and O. Wachsen, Thermal decomposition of biodegradable polyesters – II. Poly(lactic acid). *Polym. Degrad. Stab.* **43**, 329–342 (1996).
38. S. Chapple, R. Anandjiwala, and S.S. Ray, Mechanical, thermal, and fire properties of polylactide/starch blend/clay composites. *J. Therm. Anal. Calorim.* **113**, 703–712 (2013).
39. Y. Wang and C.-S. Lin, Preparation and characterization of maleated polylactide-functionalized graphite oxide nanocomposites. *J. Polym. Res.* **21**, 334(1–14) (2014).
40. D.L. Pavia, G.M. Lampman, and G.S. Kriz, Jr., *Introduction to Spectroscopy: A Guide for Students of Organic Chemistry*, pp. 1–80, Harcourt Brace Jovanovich College Publishers, Philadelphia (1979).
41. O. Persenaire, M. Alexandre, P. Degée, and P. Dubois, Mechanisms and kinetics of thermal degradation of poly(ε-caprolactone). *Biomacromolecules* **2**, 288–294 (2001). DOI: 10.1021/bm0056310
42. X. Liu, S. Khor, E. Petinakis, L. Yu, G. Simon, K. Dean, and S. Bateman, Effects of hydrophilic fillers on the thermal degradation of poly(lactic acid). *Thermochim. Acta.* **509**, 147–151 (2010).
43. X. Wu, L. Wang, C. Wu, J. Yu, L. Xie, G. Wang, and P. Jiang, Influence of char residues on flammability of EVA/EG, EVA/NG and EVA/GO composites. *Polym. Degrad. Stab.* **97**, 54–63 (2012).
44. J. Jin, Q.-X. Dong, Z.-J. Shu, W.-J. Wang, and K. He, Flame retardant properties of polyurethane/expandable graphite composites. *Procedia Eng.* **71**, 304–309 (2014).
45. Cereplast, Inc., http://trellisbioplastic.com/wp-content/uploads/2014/08/Sustainable-1001-Property-Guide.pdf (26 October 2015).